A NEW ALGORITHM FOR THE DETERMINATION OF ENERGY AND CHARGE DEPOSITION PROFILES IN VARIOUS MATERIALS RESULTING FROM ISOTROPIC ELECTRON INCIDENCE

Brian P. Beecken[1], **Shane B. Dirks**[1], **Stephen W. Gronseth**[1], **and David A. Barton**[2]

[1]*Physics Department, Bethel University, St. Paul, Minnesota, USA*
[2]*Air Force Research Laboratory, Kirtland Air Force Base, Albuquerque, New Mexico, USA*

ABSTRACT

An interpolative algorithm has been developed which produces energy and charge deposition profiles that result from isotropically incident electrons. Monte Carlo simulations using the MCNP6 transport code have been made for electrons with 40.0 keV to 5.0 MeV kinetic energies incident on thick slabs of materials with atomic numbers ranging from 6 to 47 and appropriate material densities. An electron point source near the surface of the target slab was used to simulate isotropic incidence, allowing for the inclusion of backscatter and secondary electron emission in the simulation. The new interpolative algorithm uses these specific Monte Carlo results to quickly produce energy and charge deposition profiles by scaling and interpolating the Monte Carlo simulations to produce deposition profiles for other scenarios. The resulting profiles have been confirmed by further Monte Carlo simulations. The algorithm should prove useful to modelers of deep-dielectric charging in realistic spacecraft environments.

Key words: isotropic electron incidence; energy deposition; charge deposition; Monte Carlo simulations; deposition algorithm.

1. INTRODUCTION

The study of deep-charging of dielectrics on spacecraft due to electron bombardment requires knowing the depth at which incident electrons are deposited in particular materials for given incident energies and incident angles. Furthermore, because the conductivity of a dielectric is increased by radiation induced conductivity (RIC), it is also necessary to know the depth profile of the energy deposited by the incident electrons. Ready access to good charge and energy deposition profiles will enhance understanding of experimental results and provide the basis for charging transport codes.

The spacecraft charging community has developed codes such as NUMIT [1], [2], [3], DICTAT [4], and SPIS [5] to model how charge deposited deep within a dielectric moves due to the developing field. Admittedly, such codes do not take into account complex transient behaviors caused by memory effects, aging, recombination, and other processes [6], but instead rely on the comparatively crude approximation of RIC. However, even if more comprehensive codes are developed, they will also require knowledge of the energy and charge deposition profiles for a variety of materials and incident electron energies.

Determination of deposition depth profiles has been primarily for normally incident electron beams. The most commonly used work is an algorithm created by Tabata and Ito [7] for energy deposition based on experimental studies and Monte Carlo (MC) simulations. Required inputs are the dielectric's atomic number and atomic weight, in addition to the electron beam's energy. The algorithm consists of curve fits used for effective atomic numbers from approximately 5.3 to 82 and incident energies from 100 keV to 20 MeV. Tabata *et al.* [8] and Kim *et al.* [2] [9] have expanded on this method of fitting curves to MC results. Using a similar approach of fitting curves to MC simulations, efforts have been made by Tabata *et al.* [10] to obtain charge deposition profiles. Also, Frederickson *et al.* [11] utilized Tabata's original energy deposition profile and further MC simulations to produce an algorithm. All of these approaches require the use of curve fitting parameters. More importantly, virtually all work on deposition profiles has been for normal incidence beams or on occasion for beams at certain specified angles.

In space, dielectrics are generally not going to charge due to an electron beam at normal incidence or any other single particular angle. Although the electron environment in space is typically anisotropic, it is very unlikely to be a beam. If, however, the orientation of the spacecraft is unknown or randomized, then a reasonable approximation would be isotropic electron flux. Unfortunately, virtually all MC simulations have been done for beams, and consequently there are almost no known algorithms that provide depth profiles for isotropic electron incidence. The problem is compounded by the issues of backscatter and secondary electron emission which, being angle-dependent, further complicate modeling. Without any other way to determine depth profiles, however,

modelers have been forced to adapt the normal incidence algorithms for isotropic incidence [3], but at best such an approach is very approximate.

Recently, a new approach has been proposed [12] that does isotropic MC simulations by utilizing a point source placed slightly above a material's surface. To the extent that MC simulations accurately include backscatter and secondary electron emission, such effects will then be automatically incorporated in the resulting deposition profiles. Monte Carlo simulations, however, are both difficult to set up and take a long time to run. A primary advantage of internal charging codes that model charge transport is their ability to quickly investigate various scenarios that may be of interest to a spacecraft designer. How does the threat of electrostatic discharge vary if parameters such as the material, its thickness, or the incident electron energy flux spectrum change? Setting up, running, and then incorporating MC results into such models for each possible scenario greatly diminishes their usefulness.

The present work builds on the proposal in [12] to use isotropic MC simulations as the basis for an algorithm that utilizes interpolative functions found in commercial software such as MATLAB. Monte Carlo simulations cannot be done for every possible scenario of interest. Rather than developing fitting functions that attempt to recreate the MC curves and then modify them for different parameters, the idea pursued here is to interpolate within a data set of MC curves as needed to produce deposition profiles matching the desired parameters. As pointed out in [12], straight interpolation will not work in some cases, and thus scaling routines must also be incorporated. We describe here the interpretive algorithm that has been developed and report on its predictions when compared to additional MC simulations.

2. THE MONTE CARLO DATA SET

Before an interpolative algorithm can function, there must be a set of curves between which to interpolate and scale. Such a data set was obtained through Monte Carlo simulation using the MCNP6 transport code. The MC simulation setup was identical to that described in [12] and the reader is referred to [12] for details. There are two differences. First, the prior work used the older version, MCNP5. A couple of runs were made to directly compare the earlier MCNP5 results with MCNP6. The profiles obtained were the same to within a few percent. Second, and more importantly, in the work presented here, actual mass densities were explicitly considered in all the MC simulations. In the original study, in order to isolate dependence on the atomic number, one particular mass density was used for all materials.

Tab. 1 shows the materials that were simulated using MCNP6 and form the MC data set used for the interpretive algorithm presented in the following section. For a compound material like Kapton, it is necessary to find an effective atomic number. The method used is given in [7].

Table 1. Materials used to develop the MC data set.

Material	Atomic Number Z	Density (g/cm^3)
Carbon	6	2.26
Kapton	6.36	1.42
Aluminum	13	2.643
Iron	26	7.87
Silver	47	10.49

Table 2. Incident isotropic electron energies used to develop the MC data set.

Incident Electron Energy (keV)
40, 100, 200, 500, 750, 900, 1000, 5000

In the MC simulations, electrons from a point source slightly off the material were used to simulate isotropic incidence. Each simulation was done for one electron energy for each material. The different incident energies are reported in Tab. 2. Each material was divided into 50 layers or cells for the simulation. As the incident energy was increased, the penetration depth increased. The number of layers was held at 50, but the thickness of each layer was increased so that a high percentage of the charge and energy deposited was recorded by MCNP6. For more details on the geometry and an estimate of the maximum error, see [12].

3. THE INTERPOLATIVE ALGORITHM

Once the MC data set is established, an interpolative algorithm needs to be built to enable a user to find depth profiles for materials and incident energies that are not already present in the MC data set. Within the commercial software tool MATLAB, there are two main multidimensional interpolating functions available: *griddatan* and *scatteredinterpolant*. Although these functions seem similar, only *griddatan* is capable of handling more than three independent variables. Because four independent variables will be required, *griddatan* was chosen. Effectively, *griddatan* creates a surface in five dimensions for the interpolation.

Naturally, the inputs to the algorithm must be essentially the same as the inputs to the MC simulation. These are listed in Tab. 3 for clarity. In addition to the energy of the incident electrons, the algorithm user will need to specify the atomic number, mass density, and total thickness of the dielectric. The desired spatial resolution of the interpolative algorithm deserves special mention. In all numerical algorithms, the material is divided into spatial

Table 3. Input parameters required by the interpolating algorithm.

Input Parameter	Units
Atomic number	Z
Density	g/cm^3
Depth of each spatial bin	cm
Electron energy	keV

"bins". For the MC data set, there were always 50 layers or spatial bins, but that is not a constriction on what the interpolative algorithm will produce. The user simply specifies the number of spatial bins desired and their size, which effectively determines both the thickness of the material and the spatial resolution of the resulting depth profile.

3.1. Interpolation of Depth

Interpolating to arbitrary depth values worked very well. The resulting curves, which can be seen in Fig. 1, fit smoothly within the MC data set.

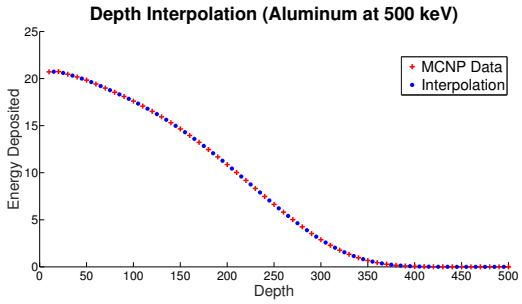

Figure 1. Interpolation to new depth bins. The algorithm outputs points that fall directly between those contained in the MC deposition data set.

3.2. Interpolation of Mass Density

Deposition profiles found with MCNP6 simulations measured depth from the surface in units of microns. Unsurprisingly, the deposition profile depths depended strongly on the mass density of the material being simulated. Certainly this situation is consistent with physical intuition; however, it made interpolation difficult. Apparently, the surface in five dimensions being interpolated over has too many irregularities. The irregularities were compounded by materials like Kapton that had a larger atomic number but lower mass density. The problem was solved by using depth measured in mass per area (g/cm^2) in the interpolation, a standard shielding parameter that is sometimes called interaction depth. Basically, the physical depth is being scaled because it is multiplied by the mass density. The result is rather consistent depths and interpolation is made relatively easy, as illustrated in Fig. 2.

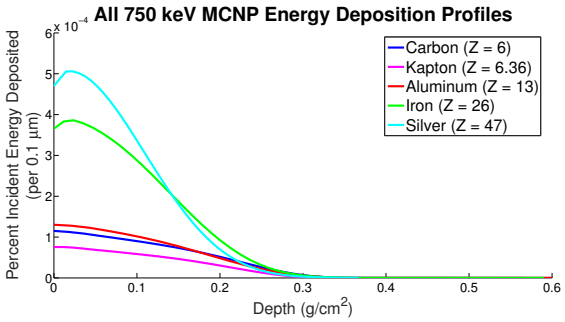

Figure 2. Plot of energy deposition profiles for all five materials in the MC data set after converting to depth measured in units of g/cm^2.

The increased consistency in profile shape is useful for interpolation, but physical interpretation is less intuitive due to differences in mass density between materials. In order to check the reasonableness of our results, we ran the interpolative algorithm for the same material at various (fictional) densities and plotted the deposition profiles as a function of distance from the surface in centimeters. Some results are shown in Fig. 3. Note the shallower penetration depth exhibited in the interpolated deposition profiles is exactly what we would expect to see with increased density.

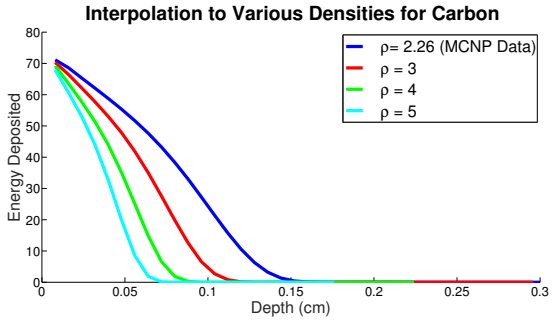

Figure 3. Deposition profiles for various densities of Carbon produced by the interpolative algorithm using the MC data set. The blue profile is a plot from the MC data set and represents deposition at the density listed in Tab. 1

3.3. Interpolation of Atomic Number

Interpolating to a new atomic number was straightforward. *Griddatan* produced curves that appeared accurate to within a reasonable margin, as can be seen in Fig. 4. The interpolated deposition curves follow the general trend of known curves and appear to be appropriately shifted relative to the atomic numbers with known deposition profiles obtained from MCNP6.

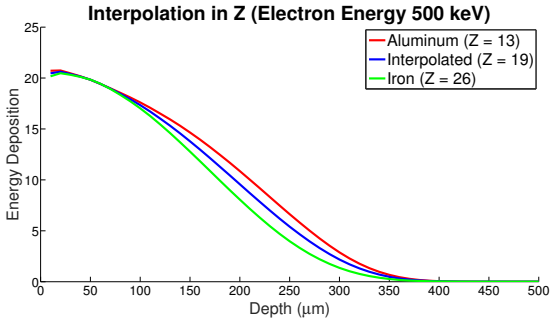

Figure 4. Interpolation to a new atomic number (Z = 19) that has no MC deposition profiles in the data set.

3.4. Interpolation of Incident Electron Energy

Interpolating to new incident electron energies proved to be far more difficult. Previous work [12] had shown that straightforward interpolation of charge and energy deposition curves for new values of electron energy resulted in deposition profiles with non-physical characteristics, as can be seen in Fig. 5. The "double peak" in the deposition profiles output by the interpolating function not only fails to follow the trends seen in the MCNP data, it implies an obviously non-physical situation. However, if we look at the interpolation from a purely mathematical standpoint, ignoring our physical intuition of what the resulting curve should look like, it is easy to see why *griddatan*, or any interpolation tool, would produce this output. Graphically, the resulting curve can be simplistically imagined as a sort of weighted average of the charge deposited at a given depth.

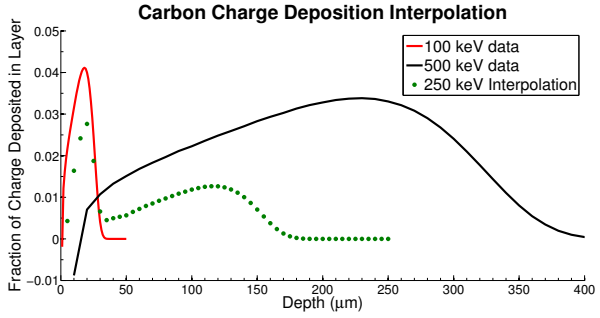

Figure 5. Simple interpolations to new incident electron energies result in the presence of a non-physical "double peak". From [12].

The poor results obtained by a direct use of *griddatan* were rectified through the implementation of a scaling subroutine (this scaling method was first proposed in [12]). First, two deposition curves were isolated from the MCNP data. The two curves that were selected had the same atomic number as the target atomic number and had incident electron energies immediately below and above the target electron energy. Having selected the data corresponding to this bracketing pair of deposition curves, the algorithm then finds the depth values corresponding to the peak in the charge deposition profiles. Assuming that the curves from the bracketing pair are close enough together that a linear relationship between peak depth and incident electron energy is appropriate (material atomic number and mass density kept constant), the algorithm uses Eq. 1 to calculate the approximate depth of the peak of the deposition curves corresponding to the target electron energy.

$$D_{\mathrm{T}} = \frac{D_{\mathrm{H}} - D_{\mathrm{L}}}{E_{\mathrm{H}} - E_{\mathrm{L}}} * (E_{\mathrm{T}} - E_{\mathrm{L}}) + D_{\mathrm{L}} \qquad (1)$$

Here D is peak depth, E is electron energy, and the subscripts T, H, and L correspond to target energy, high bracketing energy, and low bracketing energy, respectively.

The approximate depth of the peak corresponding to the target electron energy that was calculated using Eq. 1 was then used to scale the depth values of the bracketing deposition profiles to place both peaks at the same depth D_{T}. This is accomplished through the application of Eq. 2 to each depth value corresponding to the bracketing deposition profiles.

$$D_{\mathrm{S}} = \frac{D_{\mathrm{T}}}{D_{\mathrm{P}}} * D_{\mathrm{O}} \qquad (2)$$

Here subscripts O and S correspond to the original and scaled depth values, subscript P corresponds to the peak depth of the bracketing profile being scaled, and subscript T corresponds to the target peak depth.

Once this scaling was completed for the charge and energy deposition curves corresponding to both bracketing electron energies, a new data set was compiled using all of the deposition profiles contained in the MC data set, but replacing the depth data corresponding to the charge and energy deposition profiles of the bracketing energies with the new scaled values. Using this new data set, *griddatan* was able to produce deposition profiles without the "double peak" seen previously. An illustration of this process is given in Fig. 6.

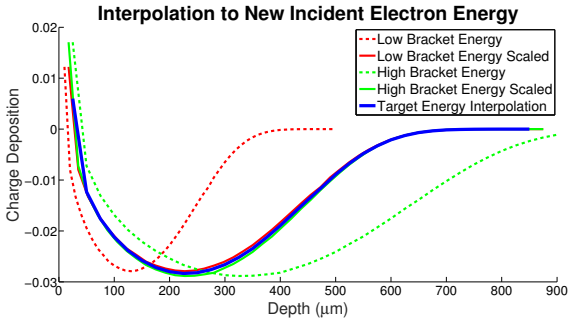

Figure 6. The dashed lines are two energy deposition profiles with incident electron energies that bracket the target energy. After scaling, the profiles are solid lines close together. The blue curve is the final interpolation to the target incident electron energy. Note that the vertical axis on charge deposition profiles can appear flipped, depending on whether or not the sign of the charge is taken into account.

Even after using the combination of scaling and interpolation just described, the deposition profiles demonstrated two additional problems. First, there often was a noticeable "ripple", which resulted from variations in the width of the depth bins in the MC data set. This subtle problem was handled by first interpolating to the target energy at a bin width consistent with the MC data, and then using the resulting profile to interpolate to the bin width input by the user. Second, after running additional MC simulations to verify the results, we found the interpolated profiles consistently overestimated the total percent energy deposited in the material. This second problem required an estimation of the correct percent energy deposited at the target incident electron energy. An appropriate approximation was made of a linear relationship between the total percent energy deposition and incident electron energy and the interpolated profiles were scaled accordingly. This scaling technique allows for the accurate interpolation to an arbitrary incident electron energy as long as the target energy falls between the minimum and maximum energies with deposition profiles present in the MCNP data set. (This condition is necessary to ensure the algorithm has access to a bracketing set of deposition profiles.) The charge deposition profile seen in Fig. 7 was obtained using this scaling method.

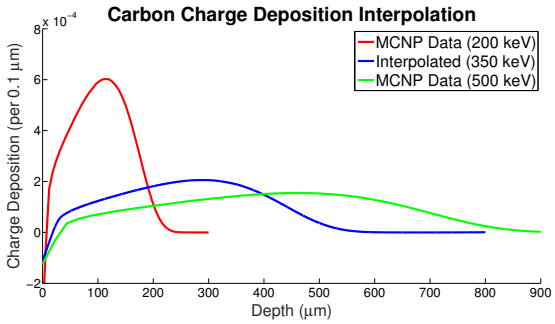

Figure 7. Interpolation to a deposition profile at a new incident energy achieved after using the scaling technique.

3.5. Simultaneous Interpolation of Electron Energy and Atomic Number

The nature of the scaling solution that was implemented to correct the interpolation to new incident electron energies necessitated the implementation of a special case to handle times when interpolation to both a new electron energy and a new atomic number was required. If there is no deposition profile data available for the desired atomic number, there are no bracketing deposition profiles to scale. In these cases the scaling algorithm is applied twice, utilizing a bracketing pair of atomic numbers with known deposition profiles, and producing two sets of deposition profiles at the target energy corresponding to the bracketing atomic numbers. These new deposition profiles are then appended to the original data set, and *griddatan* is able to utilize this data set to interpolate to the desired atomic number and electron energy.

The process is illustrated in Fig. 8. All three profiles in this plot are the result of interpolation. The profiles for aluminum and iron, both of which have deposition profiles in the MC data set, were interpolated to the target incident electron energy. These two interpolated curves were then added to the overall data set. Yet another interpolation to the atomic number produced the deposition profile for titanium, a material not in the MC data set. This method allows the new interpolative algorithm to produce accurate deposition curves for cases where there is no MC data for either the atomic number or the incident electron energy, as long as the target atomic number falls between the extremes of the atomic numbers with deposition profiles present in the MCNP data set (as a bracketing set of deposition profiles is once again necessary for the execution of the algorithm).

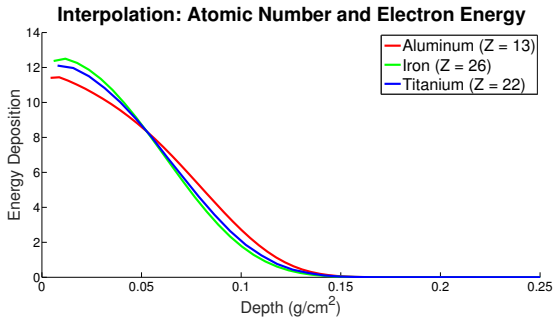

Figure 8. The combined scaling and interpolative algorithm used to find a deposition profile for a material (titanium) not in the MC data set at an incident energy (350 keV) not in the MC data set.

4. VERIFICATION OF NEW INTERPOLATIVE ALGORITHM

The deposition profiles output by the newly developed interpolative algorithm must be verified. Obviously, experimental data would be ideal, but the necessary data does not exist. Therefore, additional MCNP6 simulations were done to produce deposition profiles that are not part of the original MC data set on which the interpolative algorithm is based. The values used for these simulations were selected to specifically test the performance of the algorithm when interpolating to unknown values of parameters individually and in combinations. The possibilities are endless, so we report only some sample results which should be sufficient to illustrate the utility and accuracy of the new interpolative algorithm.

An example of an interpolation required to find deposition profiles for an incident electron energy not present in the MC data set is presented in Fig. 9 for the material iron. The correlation between the MCNP6 simulation and the new interpolative algorithm is gratifying. The closest incident electron energy available in the MC data set is different by a factor of two, and yet the algorithm produced curves that never deviate by more than a few percent from the MCNP6 simulation.

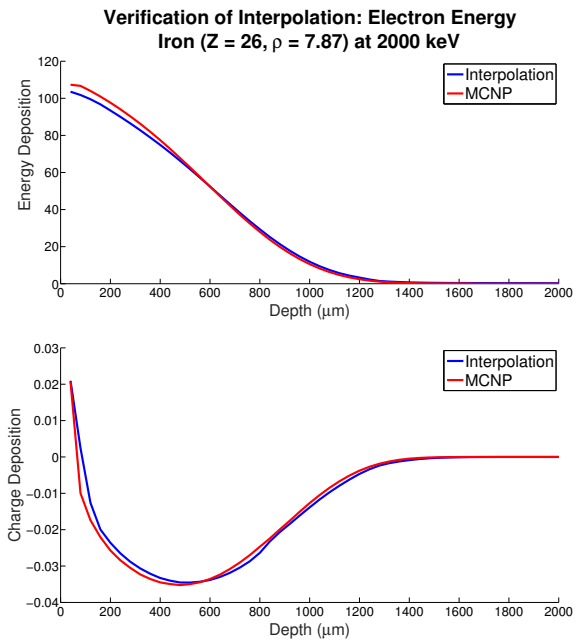

Figure 9. Deposition profiles for iron (Z = 26) with a mass density $\rho = 7.87$ g/cm^3 at an incident electron energy of 2000 keV.

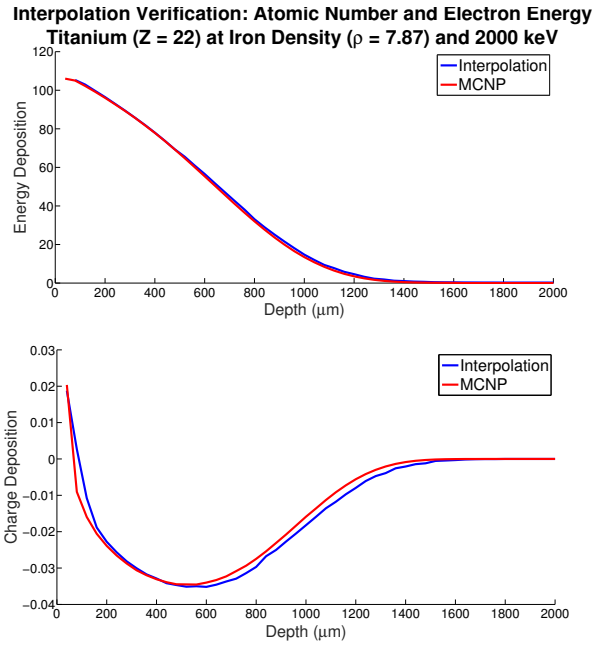

Figure 10. Deposition profiles for titanium (Z = 22) with a mass density the same as iron ($\rho = 7.87$ g/cm^3) at an incident electron energy of 2000 keV.

Next, we present an example that required the interpolative algorithm to find deposition profiles at both an atomic number and an incident electron energy that do not appear in the MC data set. For Fig. 10, the material used was titanium with atomic number 22, but the mass density was artificially kept at the density of iron. As in Fig. 9, an incident electron energy of 2000 keV was used—a value that falls between the 1000 keV and 5000 keV incident energies that are available in the MC data set. Again, the interpolative algorithm correlates very nicely to the MCNP6 simulation results.

Finally, the interpolative algorithm was used to produce deposition profiles for a material with an atomic number and a mass density that are not available in the MC data set that the algorithm is built on. Fig. 11 shows profiles for 750 keV electrons incident on titanium. Although the correlation here between the interpolative algorithm and the MCNP6 simulations appears a little less than in the previous examples, the deviation is not more than about 5%. Several other cases were tried that are not presented here, and they all showed correlation to within about 5%.

5. CONCLUSIONS

A new interpolative algorithm has been developed which allows for the quick acquisition of approximate charge and energy deposition profiles in various materials due to isotropic, high-energy electron bombardment. The algorithm is based on a data set developed from MCNP6 simulations of isotropically incident electrons with energies as low as 40 keV and as high as 5000 keV. It utilizes the *griddatan* function in MATLAB in conjunction with peak scaling techniques, total energy deposition scaling, and appropriate interaction depth units (g/cm^2). The algorithm produces deposition profiles corresponding to a broad range of parameters: atomic number, mass density, dielectric thickness, depth resolution, and incident electron energy. Energy and charge deposition profiles produced by this interpolative algorithm were found to be in very close agreement with verification profiles obtained through independent MCNP6 simulations.

Energy and charge deposition profiles for isotropically incident electrons are in short supply. To our knowledge, there is only one published attempt at comprehensive MC simulations of isotropic incidence [12], and although that attempt did not include a complete algorithm, it did lay the foundations for the approach presented in the present paper. Furthermore, the only known algorithm for predicting isotropic deposition profiles [3] is an analytical extension of a normal incidence model—admittedly a first approximation. Nevertheless, modeling of internal charging in spacecraft requires deposition profiles as a starting point. The interpolative algorithm developed here represents a significant step forward. In addition to filling a significant need, the approach is flexible enough that the algorithm can undergo significant improvement and refinement as additional MC simulations are added to the data set that the interpolative algorithm is built upon. In the future, adding Monte Carlo simulations of deposition in compound materials typically used in spacecraft would be particularly helpful and should further enhance the interpolative algorithm's usefulness for spacecraft modeling.

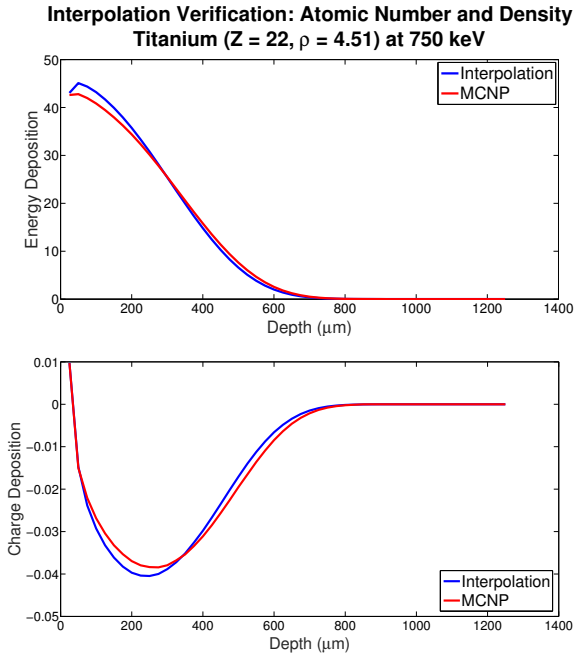

Figure 11. Deposition profiles for titanium (Z = 22 and $\rho = 4.51$ g/cm^3) at incident electron energy 750 keV.

REFERENCES

[1] Jun, I., Garrett, H.B., Kim, W. & Minow, J.I. (2008). Review of an Internal Charging Code, NUMIT, *IEEE Trans. Plasma Sci.* **36**(5), 2467–2472.

[2] Kim, W., Jun, I. & Garrett, H.B. (2012). NUMIT 2.0: the latest version of the JPL internal charging analysis code. In *Proc. of the 12th Spacecraft Charging Technology Conference* (CD-ROM), Kitakyusho, Japan.

[3] Beecken, B.P., Englund, J.T., Lake, J.J. & Wallin, B.M. (2015). Application of AF-NUMIT2 to the Modeling of Deep-dielectric Spacecraft Charging in the space Environment, *IEEE Trans. Plasma Sci.* **43**(9), 2817-2827.

[4] Rodgers, D.J., Ryden, K.A., Wrenn, G.L., Latham, P.M., Sorensen, J. & Levy, L. (1998). An Engineering Tool for the Prediction of Internal Dielectric Charging, In *Proc. of the 6th Spacecraft Charging Technology Conference*, AFRL-VS-TR-20001578, Hanscom AFB, USA, 125-130.

[5] Roussel, J.F., *et al.* (2008). SPIS open-source code: Methods, capabilities, achievements, and prospects, *IEEE Trans. Plasma Sci.* **36**(5), 2360–2368.

[6] Molinie, P. (2015). A Panorama of Electrical Conduction Models in Dielectrics, With Application to Spacecraft Charging, *IEEE Trans. Plasma Sci.* **43**(9), 2869-2874.

[7] Tabata, T. & Ito, R. (1974). An Algorithm for the Energy Deposition by Fast Electrons, *Nuclear Sci. Eng.* **53**(2), 226–239.

[8] Tabata, T., Andreo, P. & Shinoda, K. (1998). An algorithm for depth-dose curves of electrons fitted to Monte Carlo data, *Radiation Physics and Chemistry*, **53**(3), 205–215.

[9] Kim, W., Jun, I. & Garrett, H.B. (2008). An algorithm for determining energy deposition profiles in elemental slabs by low (< 100 keV) energy electrons: an internal charging application, *IEEE Trans. Nuc. Sci.* **55**(6), 3158–3163.

[10] Tabata, T., Andreo, P. & Rinsuke, I. (1994). Depth profile of charge deposition by 0.1 to 100 MeV electrons in elemental absorbers, *Nucl. Instr. Meth. Phys. Res. B*, **94**(1), 103–106.

[11] Frederickson, A.R., Bell, J.T. & Beidl, E.A. (1995). Analytic Approximation for Charge Current and Deposition by 0.1 to 100 MeV Electrons in Thick Slabs, *IEEE Trans. Nuc. Sci.* **42**(6), 1910–1921.

[12] Barton, D.A., Beecken, B.P. & Hoglund, R.M., (2015). Determination of Energy and Charge Deposition Profiles in Elemental Slabs From an Isotropically Equivalent Electron Source Using Monte Carlo simulations, *IEEE Trans. Plasma Sci.* **43**(9), 2861-2868.